Talanta 174 (2017) 521–526

Contents lists available at ScienceDirect

Talanta

journal homepage: www.elsevier.com/locate/talanta

High sensitivity surface plasmon resonance biosensor for detection of microRNA and small molecule based on graphene oxide-gold nanoparticles composites

Qing Li, Qing Wang*, Xiaohai Yang, Kemin Wang*, Hua Zhang, Wenyan Nie

State Key Laboratory of Chemo/Biosensing and Chemometrics, College of Chemistry and Chemical Engineering, Key Laboratory for Bio-Nanotechnology and Molecule Engineering of Hunan Province, Hunan University, Changsha 410082, PR China

ARTICLE INFO

Keywords:
Surface plasmon resonance
Graphene oxide-gold nanoparticles composites
MicroRNA
Adenosine

ABSTRACT

A versatile and sensitive surface plasmon resonance (SPR) biosensor based on two layers of graphene oxide-gold nanoparticles (GO-AuNPs) composites was designed for the detection of microRNA (miRNA) and small molecule adenosine. The bottom layer, which acted as a functionalized substrate on the sensor chip, provided a high specific surface area convenient for the immobilization of capture DNA molecules. The upper layer served as a signal-amplification element. By employing these two layers of GO-AuNPs composites, the dual amplification strategy was achieved so that a measurement of miRNA-141 with a detection limit of 0.1 fM was obtained. Moreover, the developed SPR biosensor showed decent selectivity toward miRNA-200 family members. Especially, the SPR biosensor demonstrated its applicability for the detection of miRNA-141 in cancer cell extractions, and the results obtained were consistent with those obtained by qRT-PCR. Interestingly, small molecule adenosine could also be detected using this SPR biosensor in combination with a split aptamer. Considering the superior sensitivity, selectivity and generality, this work promised much potential for the detection of various biomolecules.

1. Introduction

Graphene-nanoparticle composites, which graphene sheets are decorated with nanoparticles, exhibit not only unique physicochemical properties of the nanoparticles and graphene, but also additional advantages and synergistic properties [1]. Thus, it greatly augments their potential for the application in bioanalysis and biosensing. Since noble metal nanoparticles, especially gold nanoparticles (AuNPs), show unique optical and electronic properties and high biocompatibility [2], they are often used to decorate on graphene sheets, resulting in a formation of graphene oxide-gold nanoparticles (GO-AuNPs) composites [3]. Recently, it was reported that GO-AuNPs composites have been particularly well-suited for constructing various sensors, such as electrochemical sensors [4,5], fluorescence sensors [6], surface enhanced Raman scattering sensors (SERs) [7], resonance Rayleigh scattering [8] and surface plasmon resonance sensors (SPR) [9,10]. Generally, the function of GO-AuNPs composites in these sensors can be categorized into two classes. The first one, existing as a sensor substrate, could provide good biocompatibility and high surface area to significantly increase the immobilization of capture probes, resulting in a subsequent increase in sensitivity [11]. In addition, GO-AuNPs composites as a sensing interface could accelerate electron transfer [12]. Thus, they have been often successfully used in various electrochemical and optical biosensors [7,13,14]. The second one, noted as a signal amplification element, also markedly increased the sensitivity of the biosensor. Zhou et al. reported a novel sandwich-type electrochemiluminescence (ECL) immunosensor for HIV-1 p24 antigen detection using GO-AuNPs and Ru(bpy)32+-dopped silica nanoparticles [15]. The GO-AuNPs composite improved the loading of ECL molecules, resulting in an increase of ECL response and a high sensitivity. We also used GO-AuNPs composites as the signal amplification element to develop a simple and sensitive SPR biosensor [9]. Whether GO-AuNPs composite acted as the sensing substrate or the signal element, it could improve the sensitivity of the biosensor. Therefore, it was speculated that the combination of these two factors can further build a high sensitivity sensor.

On the basis of our previous work, a novel and sensitive SPR biosensor based on two layers of GO-AuNPs composites was developed. As far as we known, this was the first report in which GO-AuNPs composites acted as not only the sensing substrate but also the signal amplification element. This approach was conducted in two simple steps as shown in Fig. 1. First, thiolated capture DNA was covalently

* Corresponding authors.
E-mail addresses: wwqq99@hnu.edu.cn (Q. Wang), kmwang@hnu.edu.cn (K. Wang).

http://dx.doi.org/10.1016/j.talanta.2017.06.048
Received 10 March 2017; Received in revised form 12 June 2017; Accepted 18 June 2017
Available online 19 June 2017

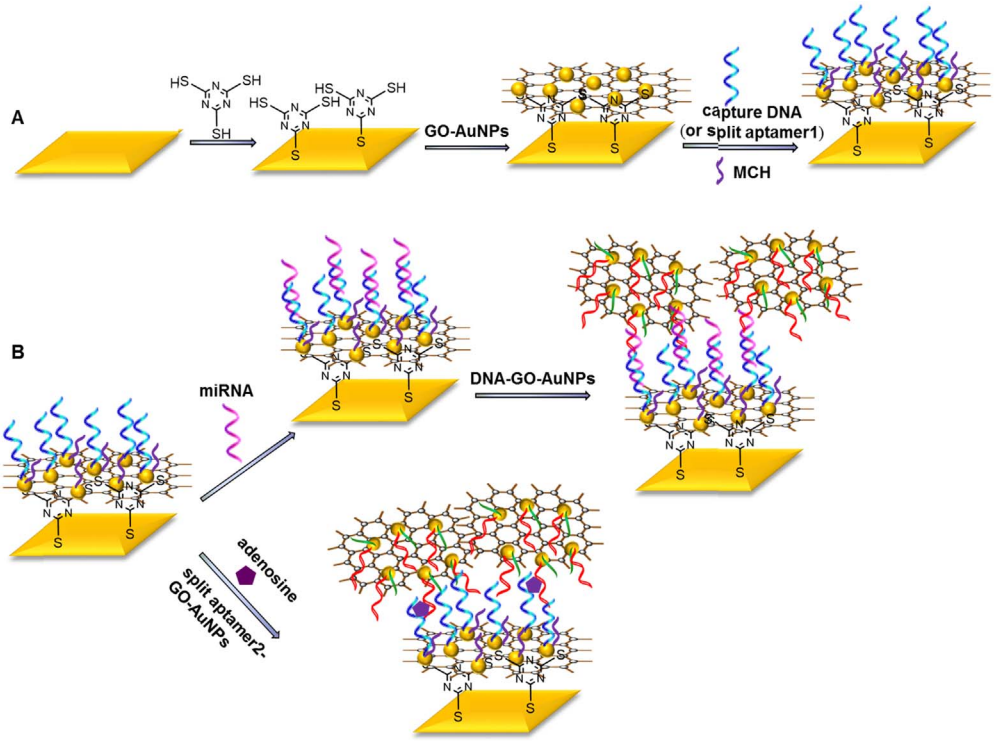

Fig. 1. Schematic illustration of the SPR biosensor based on the GO-AuNPs composites.

attached to the GO-AuNPs functionalized Au film surface (shown in Fig. 1A). In the second step, target miRNA and DNA functionalized GO-AuNPs composites (DNA-GO-AuNPs) were respectively introduced, and then the sandwich structure was formed due to DNA/RNA hybridization (shown in Fig. 1B). In this step, target miRNA was recognized, and the two layers of GO-AuNPs were used to enhance the SPR response. Accordingly, target miRNA was detected sensitively. More importantly, on the basis of split aptamers, another target, small molecule adenosine, was also detected using this approach. An aptamer for adenosine was first designed in two flexible ssDNA pieces. One (i.e. split aptamer1) was tethered on the GO-AuNPs functionalized Au film and the other (i.e. split aptamer2) was modified on the GO-AuNPs composites. In the presence of adenosine, the GO-AuNPs labelled adenosine-aptamer complex was formed since the two split aptamers reassembled into an intact aptamer structure. By employing the GO-AuNPs amplification strategy, target adenosine could also be detected sensitively. Theoretically, this approach was potentially used for various types of target detection, on condition that the appropriate probe can be found and replaced.

2. Experimental

2.1. Materials and reagents

Chloroauric acid ($HAuCl_4 \cdot 4H_2O$), trisodium citrate and diethylpyrocarbonatex (DEPC) were obtained from Shanghai Reagent Company (Shanghai, China). Thiocyanuric acid, 6-mercapto-1-hexanol (MCH), adenosine, uridine, cytidine and guanosine were purchased from Sigma (USA). DNA oligonucleotides and RNA oligonucleotides (shown in Table 1) were synthesized by Shanghai Sangon Biotechnology Co. (Shanghai, China) and TaKaRa Biotechnology Co. (Dalian, China), respectively. Ultrapure water (18.2 MΩ cm) was prepared using a Millipore system (Millipore, USA). All oligonucleotides were dissolved into 10 mM PBS buffer (pH 7.4) containing 100 mM NaCl. All solutions used were protected from RNase degradation through DEPC treatment.

Table 1
Sequences of all oligonucleotides used.

Name	Sequence
Capture DNA	5′-AGA CAG TGT TAT TTT TTT TTT-SH-3′
Assistant DNA	5′-SH-TTT TTT TTT TTT TCC ATC TTT ACC-3′
Helper DNA	5′-SH-TTT TTT TTT TTT T–3′
miRNA-141	5′-UAACACUGUCUGGUAAAGAUGG-3′
miRNA-429	5′-UAAUACUGUCUGGUAAAACCGU-3′
miRNA-200a	5′-UAACACUGUCUGGUAACGAUGU-3′
miRNA-21	5′-UAGCUUAUCAGACUGAUGUUGA-3′
Random miRNA	5′-N_{22}-3′
Split aptamer1	5′-SH-TTT TTT TTT TAC CTG GGG GAG TAT-3′
Split aptamer2	5′-SH-TTT TTT TTT TTG CGG AGG AAG GT-3′

2.2. Synthetization and modification of graphene oxide (GO)-gold nanoparticles (AuNPs) composites

The GO-AuNPs composites were synthetized as described in the previous work [9,16]. Briefly, after $HAuCl_4$ solution (0.48 mM) was mixed with GO solution (1 mg mL^{-1}) for 30 min at room temperature, the mixture was heated to 80 °C. Next, sodium citrate (1.6 mM) was added dropwise. After incubation for 60 min, the mixture was centrifuged at 5000 rpm for 15 min, and the resultant precipitate was rinsed with water to remove free AuNPs. GO-AuNPs composites were characterized by TEM. It showed that Au nanoparticles with an average size of 18 ± 2 nm was observed at the GO surface (Fig. S1, Supporting information).

DNA functionalized GO-AuNPs composites (DNA-GO-AuNPs) were obtained according to our previous work [9]. In brief, the mixture of assistant DNA (or split aptamer2) and helper DNA was incubated with GO-AuNPs composites solution for 16 h at 4 °C. Next, the solution was aged in 10 mM phosphate buffer (pH 7.0, 100 mM NaCl) for 40 h at 4 °C. After the solution was centrifuged at 13,500 rpm for 20 min, the precipitate was washed twice using 10 mM phosphate buffer (pH 7.0, 100 mM NaCl). Finally, DNA-GO-AuNPs were obtained and dispersed in 10 mM phosphate buffer (pH 7.0, 100 mM NaCl). The DNA-GO-

AuNPs composites can be stored at 4 °C over two weeks, indicating it had a good stability.

GO-AuNPs composites and DNA-GO-AuNPs were characterized using UV–visible spectrophotometer (UV-1601, Shimadzu), respectively. As shown in Fig. S2 of Supporting information, GO-AuNPs composites possessed two absorption peaks at 230.0 and 524.0 nm, which was associated with the presence of GO and AuNPs, separately. For DNA-GO-AuNPs, the absorption peak at 524.0 nm shifted to 528.0 nm, implying that DNA was modified on the GO-AuNPs composites.

2.3. Surface modification of Au film

Au film was first cleaned according to the previous works [9,17]. Then, it was modified with 20 mM thiocyanuric acid for 3 h at room temperature, followed by rinsing in running PBS buffer (pH 7.4, 10 mM). Next, GO-AuNPs composites were injected. After incubated for 3 h at room temperature, the Au film was washed with PBS buffer repeatedly. GO-AuNPs composites can be immobilized on Au film surfaces stably through the Au-S bonds. Subsequently, the GO-AuNPs functionalized Au film was incubated with 5 μM capture DNA (or split aptamer1) for 3 h at room temperature, followed by washing in 10 mM PBS buffer (pH 7.4). For reducing nonspecific binding of capture DNA and controlling the orient of DNA on the Au film, the Au film was treated with 1 mM MCH for 30 min at room temperature. After rinsing with PBS buffer repeatedly, a sensor chip was prepared.

The surface modification of Au film was characterized using a commercially available EC-SPR1010 device (Changchun Dingcheng Technology, China). The resonance angle change, which was larger than 0.0015°, was acted as a signal for this SPR instrument. As shown in Fig. S3 (Supporting information), after incubated with GO-AuNPs composites, SPR spectrum changed from curve 1 to curve 2 and an obvious resonance angle shift (0.0838°) was observed. Then, as the capture DNA and MCH were injected respectively, SPR spectrum changed to curve 3 and resonance angle increased to 0.2159°. It was suggested that the capture DNA was immobilized on the Au film. In addition, Au film in the absence and presence of GO-AuNPs composites was characterized using scanning probe microscope (SP13800NSPA400, Seiko, Japan). As shown in Fig. S4 of the Supporting information, GO-AuNPs composites were successfully modified on the Au film surface.

2.4. Detection of miRNA

MiRNA solution of different concentrations was injected and incubated with the capture DNA immobilized on the sensor chip for 50 min at room temperature, then rinsed using 10 mM PBS thoroughly. Next, DNA-GO-AuNPs were injected and reacted for 1 h at room temperature, followed by a thorough rinsing with 10 mM PBS. The concentration of miRNA was determined through to the change of resonance angle. Here, regeneration of the sensor chip was achieved using 0.1% SDS / 10 mM NaOH.

The total RNA was first extracted from human cancer cell lines using Trizol reagent (Sangon Co. Ltd., Shanghai, China) according to the manufacturer's instructions. Then, the pure and concentrated RNA was divided into two equal parts for analysis using qRT-PCR and the SPR biosensor. The cDNA samples were synthesized using the reverse transcription (RT) reaction with AMV First Strand cDNA Synthesis Kit (BBI, Toronto, Canada). Then the transcribed cDNA was acted as the template for qRT-PCR. qPCR analysis of miRNA was achieved with SG Fast qPCR Master Mix(2X) (BBI), according to the indicated protocol on an LightCycler480 Software Setup (Roche).

2.5. Detection of adenosine

Detection of adenosine was achieved by exposing the sensor chip to the mixture solution of split aptamer2 functionalized GO-AuNPs and different concentration of adenosine for 1 h at room temperature, then rinsed using 10 mM PBS thoroughly. Adenosine could be quantified through the shift of resonance angle. Similarly, the sensor chip was regenerated using 0.1% SDS / 10 mM NaOH.

3. Results and discussions

3.1. MiRNA detection using SPR biosensor based on GO-AuNPs composites

The feasibility of the SPR biosensor based on GO-AuNPs composites was first investigated. As described in Fig. 2A, when 10 pM miRNA-141 was injected, SPR spectrum changed from curve 1 to curve 2 and a small change of the resonance angle (0.0119°) was achieved, suggesting that miRNA was recognized. After incubation with DNA-GO-AuNPs, it gave an obvious resonance angle shift by 0.1744° (curve 3), indicating that DNA-GO-AuNPs were associated with the capture DNA/miRNA complex. In this process, there were at least 3 reasons for the amplification of SPR response. First, the surface plasmon of AuNPs on the surface of GO sheet might have been resonantly excited through energy transfer in the near field and have created a strong local electromagnetic field, which enhanced the SPR response [18]. The high mass-density and dielectric constant of the AuNPs on the surface of GO sheets also improved the SPR response. Second, the electromagnetic coupling between the AuNPs on the upper layer of GO-AuNPs composites and the underlying Au film could enhance the SPR response [19,20]. Third, the bottom GO-AuNPs could immobilize many capture DNA molecules due to its high specific surface area, so more DNA-GO-AuNPs could be captured on the sensor chip [12]. Subsequently, the SPR response was further amplified. After the sensor chip was reacted with 0.1% SDS / 10 mM NaOH, SPR spectrum shifted from curve 3 to curve 4, and the resonance angle of curve 4 was almost consistent with that of curve 1. The results indicated that the sensor chip was regenerated.

Different concentrations of miRNA-141 were then tested. As seen in Fig. 2B, the resonance angle increased following the increase of the miRNA-141 concentration, implying that the increased quantity of DNA-GO-AuNPs was captured on the sensor chip. The relation between the change of resonance angle (Δθ) and the miRNA-141 concentration was summarized in Fig. 2B. Given that the resonance angle change which was larger than 0.0015° acted as a signal, it was found that the detection limit of two layers of GO-AuNPs enhanced SPR (curve a) was 0.1 fM. Recently, we utilized one layer of GO-AuNPs composites as a signal amplification element to develop a simple and sensitive SPR biosensor [9]. Comparatively speaking, the detection limit of two layers of GO-AuNPs enhanced SPR (curve a) was 1 order of magnitude lower than that of one layer of GO-AuNPs enhanced SPR (curve b). Presumably, compared with the Au film in one layer of GO-AuNPs enhanced SPR, the bottom GO-AuNPs could immobilize more capture DNA molecules due to its high specific surface area, and more DNA-GO-AuNPs could be captured on the sensor chip accordingly. Moreover, the sensitivity of two layers of GO-AuNPs enhanced SPR was higher than those of previous works [9,17,21–29].

Subsequently, different concentrations solutions of miRNA-200a, miRNA-429, miRNA-21 and random miRNA were used to evaluate the selectivity of this SPR biosensor. Amongst these miRNAs, miRNA-141, miRNA-200a and miRNA-429 are members of the miRNA-200 family. As expected in Fig. 2C, for random miRNA and miRNA-21, there was no increase in SPR signal. Compared with target miRNA-141, Δθ increased slightly following the increase of miRNA concentration for

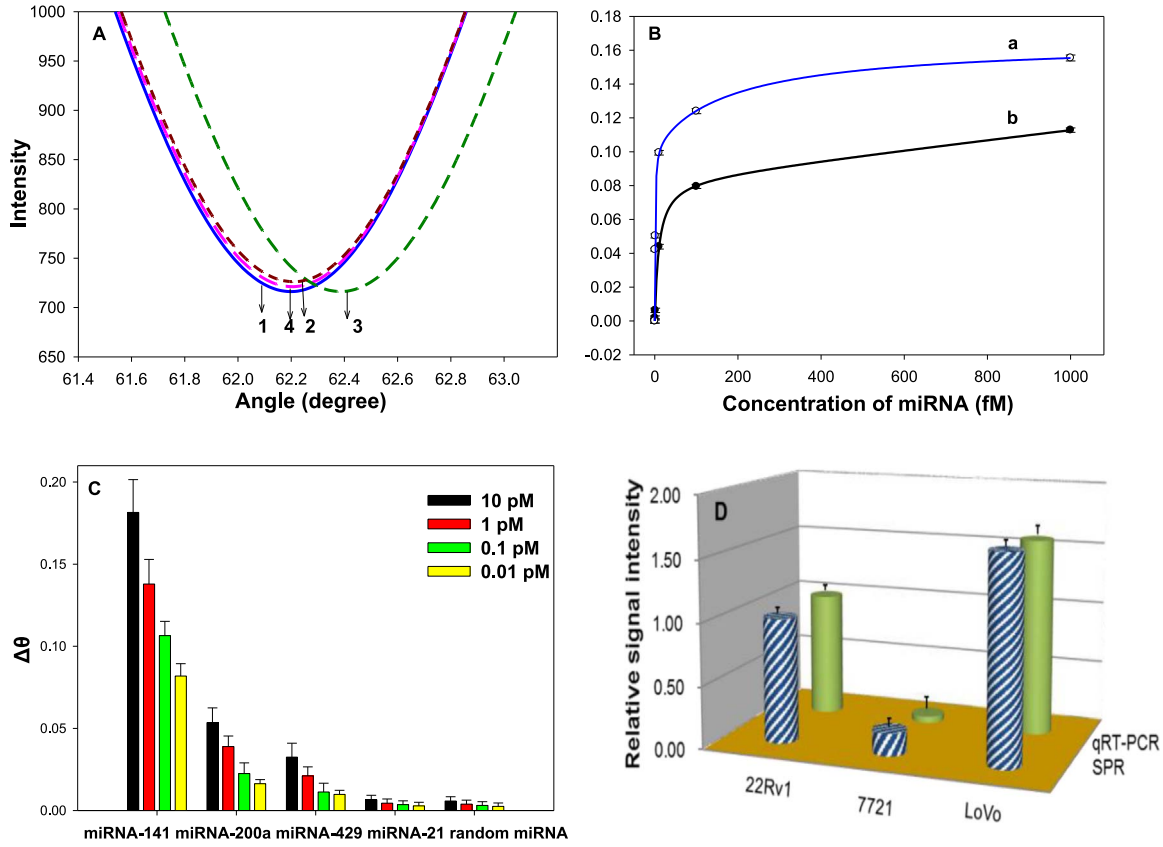

Fig. 2. (A) SPR spectra of (1) capture DNA modified on the GO-AuNPs functionalized Au film; (2) hybridization with 10 pM miRNA-141; (3) reaction with the DNA-GO-AuNPs; (4) regeneration. (B) The relationship between Δθ and miRNA-141 concentrations by using (a) two layers of GO-AuNPs enhanced SPR and (b) one layer of GO-AuNPs enhanced SPR. (C) Selectivity investigation of the two layers of GO-AuNPs enhanced SPR biosensor. (D) Paired comparison of the miRNA-141 levels detected in total RNA isolated from three human cancer cell lines using the SPR biosensor (blue histogram) or qRT-PCR (green histogram). Relative signal intensity was based on the expression ratio of miRNA-141 in target cell lines versus that in 22Rv1 cell lines. Error bars showed the standard deviation of measurement taken from three experiments.

miRNA-200a and miRNA-429. Take 1 pM miRNA as a case, Δθ was 0.1379° for miRNA-141, which was seven times larger than that of miRNA-429 and four times larger than that of miRNA-200a. Moreover, the selectivity of the biosensor including compounds was also investigated. As shown in Fig. S5 of the Supporting information, a clear response was observed in case of target miRNA-141 (1 pM) or a mix of three miRNAs while slightly signal was observed for either miRNA-200a (10 pM) or miRNA-429 (10 pM). The response caused by miRNA-141 was similar to that caused by the mix of three miRNAs, implying that miRNA-200a and miRNA-429 did not interfere the detection of target miRNA-141. It clearly showed that distinct sequence specificity was achieved using the SPR biosensor.

Given the excellent selectivity of this SPR system, target miRNA-141 in three human cancer cell lines, i.e. prostate carcinoma cell lines (22Rv1), hepatocellular carcinoma cell lines (SMMC-7721), and colon cancer cell lines (LoVo), were also measured using the SPR biosensor. According to our previous work [9], miRNA-141 levels were defined using the relative expression levels based on the expression ration of miRNA-141 in cell lines versus that in 22Rv1 cell lines. The relative expression levels of miRNA-141 were measured by two technologies, i.e. qRT-PCR and the developed SPR biosensor. Interestingly, those two technologies generated a similar result that it had different miRNA-141 expression levels in those three cancer cell lines. As described in Fig. 2D, the cell extractions from the 22Rv1 cell and the LoVo cell had a higher miRNA concentration than that of the SMMC-7721 cell. This result was consistent with the previous studies that reported that miRNA-141 expressed in a wide range of common cancers including colon and prostate cancer [9,30]. As can be seen, the developed SPR has considerable promise for practical applications in miRNA detection.

3.2. Analytical performance of adenosine detection

Besides miRNA, small molecules were also detected using the above mentioned SPR biosensor combined with the split aptamer. Here, adenosine was chosen as the model. Likewise, the feasibility of adenosine detection was first analyzed. As described in Fig. 3A. After the mixture solution of 2 nM adenosine and split aptamer2 functionalized GO-AuNPs was reacted with split aptamer1 immobilized on the sensor chip, a huge resonance angle shift was observed (from curve 1 to curve 2), indicating the formation of adenosine/aptamer complex on the sensor chip. When the sensor chip was treated using 0.1% SDS/10 mM NaOH, SPR spectrum shifted from curve 2 to curve 3, and the resonance angle of curve 3 was basically consistent with that of curve 1. It was suggested that regeneration of the sensor chip was achieved. In addition, as only adenosine or split aptamer2 functionalized GO-AuNPs was injected, almost no SPR response was monitored, implying that no adenosine/aptamer complex was assembled on the sensor chip.

Next, different concentration of adenosine was detected. As shown in Fig. 3B, the SPR response increased with the increase of adenosine concentration, due to the increased quantity of adenosine/aptamer complex on the sensor chip. As shown in the inset of Fig. 3B, it illustrated a good linear relationship between the logarithms of adenosine concentrations and the shift of resonance angle over a range of 0.1 pM to 2.0 nM. The calibration equation was $\Delta\theta = 0.024\text{Log } C + 0.0991$ ($R^2 = 0.9887$) (Δθ was the change of resonance angle, and C was the concentration of adenosine). Since a change of resonance angle larger than 0.0015° was defined as a signal, the detection limit of the SPR sensor was calculated to be 0.1 pM, which was notably lower than that of the previous works [20,27,31–38].

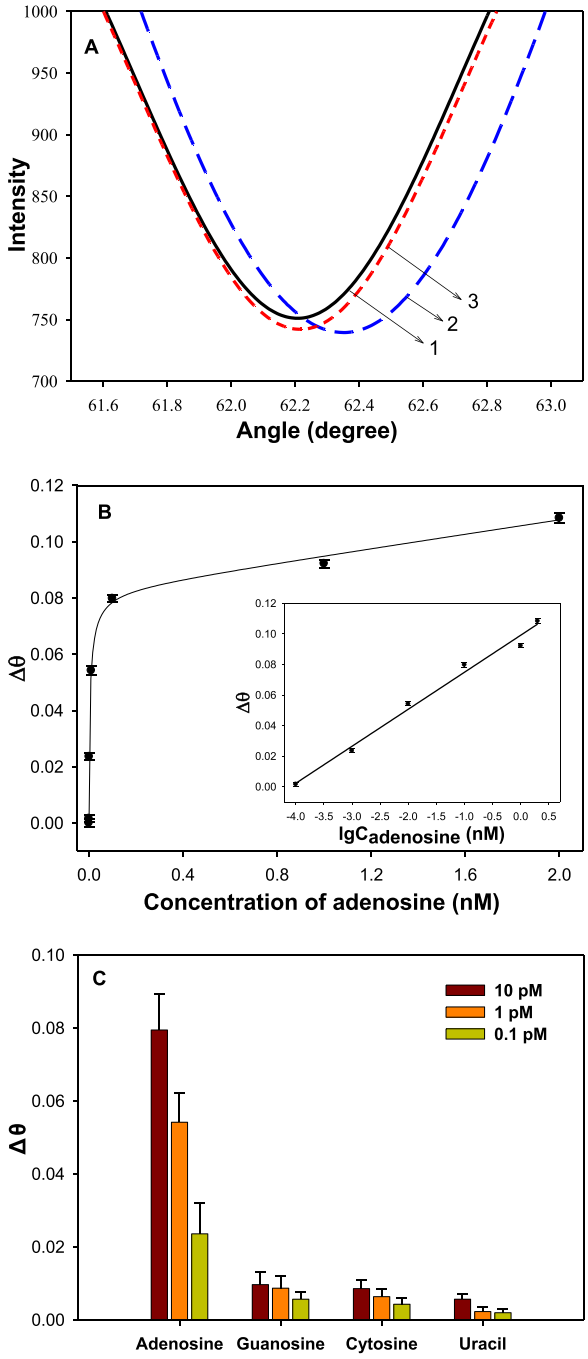

Fig. 3. (A) SPR spectra of (1) split aptamer1 modified on the GO-AuNPs functionalized Au film; (2) reaction with the mixture of 2 nM adenosine and DNA-GO-AuNPs; (3) regeneration. (B) The relationship between Δθ and adenosine concentrations. Error bars showed the standard deviation of measurement taken from three experiments. (C) Selectivity investigation. Error bars showed the standard deviation of measurement taken from three experiments.

Moreover, adenosine analogue solutions of uridine, cytidine, and guanosine were selected as contrasts for the investigation of the selectivity of this system. As described in Fig. 3C, for three adenosine analogue, all of the resonance angle changes were significantly lower than that caused by adenosine, suggesting that the split aptamers still showed excellent selectivity for adenosine. Take 100 pM adenosine and adenosine analogue as an example, Δθ was 0.0795° for adenosine, which was more than thirteen times larger than that of uridine, nine times larger than that of cytidine, and eight times larger than that of guanosine. The results clearly showed that the SPR biosensor had decent selectivity for adenosine detection.

Table 2
Detection of adenosine in diluted human serum samples.

	C1 / pM	ΔC / pM	C2 / pM	Rate of recovery / %
Sample 1	66.5	20.0	86.7	101.0
Sample 2	66.5	60.0	126.5	100.0
Sample 3	66.5	90.0	156.0	99.4

C1: concentration determined in unfortified sample; ΔC: concentration of fortification; C2: concentration determined in fortified sample. Rate of recovery (%) = ((C2-C1) / ΔC) × 100%.

To test the applicability and reliability of the presented SPR biosensor, the SPR biosensor was used to analyze adenosine in diluted human serum. Since adenosine concentration in normal human blood plasma ranges between 50 nM and 100 nM [39], the human serum samples were diluted 1000 times with buffer (10 mM PBS, pH 7.4). Then difference concentrations of adenosine were added in diluted serum samples for preparing the adenosine-spiked serum samples. Finally, these samples were filtered to remove macromolecules using centrifugal filtration devices (MWCO = 10,000 Da, Millipore) for minimize nonspecific adsorption. As shown in Table 2, recovery of adenosine from diluted human serum samples was 99.4–101.0%. These results indicated that the present SPR sensor could be practically applied in clinical adenosine detection analysis.

4. Conclusion

In conclusion, a novel, sensitive and versatile GO-AuNPs composites-based SPR biosensor was introduced. In this biosensor, two layers of GO-AuNPs was utilized for signal amplification. The bottom layer, which was functionalized on Au film, had a large specific surface area so that it could immobilize more capture DNA molecules, resulting in the amplification of SPR response. The upper layer, which acted as a signal-enhancing label, could further enhance the SPR response. Employing two layers of GO-AuNPs amplification strategy, the SPR biosensor showed superior sensitivity. In addition, the SPR biosensor exhibited reasonable selectivity and it could be effectively applied to complex systems, such as cancer cell extraction and serum. Significantly, this approach can be potentially used for the detection of a wide variety of targets such as proteins, cells, and other small molecules, as long as the appropriate probe can be found and replaced. This work provided a promising avenue for bioanalysis and biosensing.

Acknowledgment

This work was supported by the National Natural Science Foundation of China (Grant: 21375034, 21675047 and 21190040), and Natural Science Foundation for Distinguished Young Scholars of Hunan Province (Grant: 2016JJ1008).

Appendix A. Supplementary material

Supplementary data associated with this article can be found in the online version at http://dx.doi.org/10.1016/j.talanta.2017.06.048.

References

[1] P.T. Yin, S. Shah, M. Chhowalla, K.B. Lee, Design, synthesis, and characterization of graphene-nanoparticle hybrid materials for bioapplications, Chem. Rev. 115 (2015) 2483–2531.
[2] J. Zhang, J.P. Lei, R. Pan, C.A. Leng, Z. Hu, H.X. Ju, In situ assembly of gold nanoparticles on nitrogen-doped carbon nanotubes for sensitive immunosensing of microcystin-LR, Chem. Commun. 47 (2011) 668–670.
[3] B.S. Kong, J.X. Geng, H.T. Jung, Layer-by-layer assembly of graphene and gold nanoparticles by vacuum filtration and spontaneous reduction of gold ions, Chem. Commun. 16 (2009) 2174–2176.
[4] N.R. Nirala, S. Abraham, V. Kumar, S.A. Pandey, U. Yadav, M. Srivastava, S.K. Srivastava, V.N. Singh, A.M. Kayastha, A. Srivastava, Partially reduced

graphene oxide–gold nanorods composite based bioelectrode of improved sensing performance, Talanta 144 (2015) 745–754.
[5] D. Zhao, Y. Wang, G. Nie, Electrochemical immunosensor for the carcinoembryonic antigen based on a nanocomposite consisting of reduced graphene oxide, gold nanoparticles and poly(indole-6-carboxylic acid), Microchim. Acta 183 (2016) 2925–2932.
[6] X. Fu, T. Lou, Z. Chen, M. Lin, W. Feng, L. Chen, "Turn-on" fluorescence detection of lead ions based on accelerated leaching of gold nanoparticles on the surface of graphene, ACS Appl. Mater. Interfaces 4 (2012) 1080–1086.
[7] J. Cheng, X. Su, S. Wang, Y. Zhao, Highly sensitive detection of clenbuterol in animal urine using immunomagnetic bead treatment and surface-enhanced raman spectroscopy, Sci. Rep. 6 (2016) 32637.
[8] Y. Wang, X. Zhang, Q. Liu, G. Wen, A. Liang, Z. Jiang, A simple and sensitive graphene oxide/gold nanoparticle surface plasmon resonance Rayleigh scattering-energy transfer analytical platform for detection of iodide and H2O2, RSC Adv. 5 (2015) 9272–9277.
[9] Q. Wang, Q. Li, X.H. Yang, K.M. Wang, S.S. Du, H. Zhang, Y.J. Nie, Graphene oxide-gold nanoparticles hybrids-based surface plasmon resonance for sensitive detection of microRNA, Biosens. Bioelectron. 77 (2016) 1001–1007.
[10] T. Yao, X. Gu, T. Li, J. Li, J. Li, Z. Zhao, J. Wang, Y. Qin, Y. She, Enhancement of surface plasmon resonance signals using a MIP/GNPs/rGO nano-hybrid film for the rapid detection of ractopamine, Biosens. Bioelectron. 75 (2016) 96–100.
[11] D. Feng, L. Li, X. Han, X. Fang, X. Li, Y. Zhang, Simultaneous electrochemical detection of multiple tumor markers using functionalized graphene nanocomposites as non-enzymatic labels, Sens. Actuators B 201 (2014) 360–368.
[12] M. Govindhan, M. Amiri, A. Chen, Au nanoparticle/graphene nanocomposite as a platform for the sensitive detection of NADH in human urine, Biosens. Bioelectron. 66 (2015) 474–480.
[13] F. Yang, Z. Yang, Y. Zhuo, Y. Chai, R. Yuan, Ultrasensitive electrochemical immunosensor for carbohydrate antigen 19-9 using Au/porous graphene nanocomposites as platform and Au@Pd core/shell bimetallic functionalized graphene nanocomposites as signal enhancers, Biosens. Bioelectron. 66 (2015) 356–362.
[14] J. Zhang, Y. Sun, B. Xu, H. Zhang, Y. Gao, H. Zhang, D. Song, A novel surface plasmon resonance biosensor based on graphene oxide decorated with gold nanorod-antibody conjugates for determination of transferrin, Biosens. Bioelectron. 45 (2013) 230–236.
[15] L. Zhou, J. Huang, B. Yu, Y. Liu, T. You, A novel electrochemiluminescence immunosensor for the analysis of HIV-1 p24 antigen based on P-RGO@Au@Ru-SiO_2 composite, ACS Appl. Mater. Interfaces 7 (2015) 24438–24445.
[16] G. Goncalves, P.A.A.P. Marques, C.M. Granadeiro, H.I.S. Nogueira, M.K. Singh, J. Grácio, Surface modification of graphene nanosheets with gold nanoparticles: the role of oxygen moieties at graphene surface on gold nucleation and growth, Chem. Mater. 21 (2009) 4796–4802.
[17] Q. Wang, R.J. Liu, X.H. Yang, K.M. Wang, J.Q. Zhu, L.L. He, Q. Li, Surface plasmon resonance biosensor for enzyme-free amplified microRNA detection based on gold nanoparticles and DNA supersandwich, Sens. Actuators B 223 (2016) 613–620.
[18] J. Zhang, Y. Sun, Q. Wu, H. Zhang, Y. Bai, D. Song, A protein A modified Au-graphene oxide composite as an enhanced sensing platform for SPR-based immunoassay, Analyst 138 (2013) 7175–7181.
[19] Q. Wang, J.H. Huang, X.H. Yang, K.M. Wang, L.L. He, X.P. Li, C.Y. Xue, Surface plasmon resonance detection of small molecule using split aptamer fragments, Sens. Actuators B 156 (2011) 893–898.
[20] B. Wu, R. Jiang, Q. Wang, J. Huang, X.H. Yang, K.M. Wang, W.S. Li, N.D. Chen, Q. Li, Detection of C-reactive protein using nanoparticle-enhanced surface plasmon resonance using an aptamer-antibody sandwich assay, Chem. Commun. 52 (2016) 3568–3571.
[21] J.B. Li, P.H. Lei, S.J. Ding, Y. Zhang, J.R. Yang, Q. Cheng, Y.R. Yan, An enzyme-free surface plasmon resonance biosensor for real-time detecting microRNA based on allosteric effect of mismatched catalytic hairpin assembly, Biosens. Bioelectron. 77 (2016) 435–441.
[22] R.J. Liu, Q. Wang, Q. Li, X.H. Yang, K.M. Wang, W.Y. Nie, Surface plasmon resonance biosensor for sensitive detection of microRNA and cancer cell using multiple signal amplification strategy, Biosens. Bioelectron. 87 (2017) 433–438.
[23] W. Cai, S. Xie, Y. Tang, Y. Chai, R. Yuan, J. Zhang, A label-free electrochemical biosensor for microRNA detection based on catalytic hairpin assembly and in situ formation of molybdophosphate, Talanta 163 (2017) 65–71.
[24] H. Vaisocherova, H. Sipova, I. Visova, M. Bockova, T. Springer, M.L. Ermini, X. Song, Z. Krejcik, L. Chrastinova, O. Pastva, K. Pimková, M.D. Merkerová, J.E. Dyr, J. Homola, Rapid and sensitive detection of multiple microRNAs in cell lysate by low-fouling surface plasmon resonance biosensor, Biosens. Bioelectron. 70 (2015) 226–231.
[25] H. Zhang, Q. Wang, X. Yang, K. Wang, Q. Li, Z. Li, L. Gao, W. Nie, Y. Zheng, An isothermal electrochemical biosensor for the sensitive detection of microRNA based on a catalytic hairpin assembly and supersandwich amplification, Analyst 142 (2017) 389–396.
[26] K. Hao, Y. He, H. Lu, S. Pu, Y. Zhang, H. Dong, X. Zhang, High-sensitive surface plasmon resonance microRNA biosensor based on streptavidin functionalized gold nanorods-assisted signal amplification, Anal. Chim. Acta 954 (2017) 114–120.
[27] X. Ding, W. Cheng, Y. Li, J. Wu, X. Li, Q. Cheng, S. Ding, An enzyme-free surface plasmon resonance biosensing strategy for detection of DNA and small molecule based on nonlinear hybridization chain reaction, Biosens. Bioelectron. 87 (2017) 345–351.
[28] S. Fang, H.J. Lee, A.W. Wark, R.M. Corn, Attomole microarray detection of microRNAs by nanoparticle-amplified SPR imaging measurements of surface polyadenylation reactions, J. Am. Chem. Soc. 128 (2006) 14044–14046.
[29] N. Nasheri, J. Cheng, R. Singaravelu, P. Wu, M.T. McDermott, J.P. Pezacki, An enzyme-linked assay for the rapid quantification of microRNAs based on the viral suppressor of RNA silencing protein p19, Anal. Biochem. 412 (2011) 165–172.
[30] B.C. Yin, Y.Q. Liu, B.C. Ye, One-step, multiplexed fluorescence detection of microRNAs based on duplex-specific nuclease signal amplification, J. Am. Chem. Soc. 134 (2012) 5064–5067.
[31] H. Huang, S. Shi, X. Gao, R. Gao, Y. Zhu, X. Wu, R. Zang, T. Yao, A universal label-free fluorescent aptasensor based on Ru complex and quantum dots for adenosine, dopamine and 17β-estradiol detection, Biosens. Bioelectron. 79 (2016) 198–204.
[32] L. Chen, Q. Cai, F. Luo, X. Chen, X. Zhu, B. Qiu, Z. Lin, G. Chen, A sensitive aptasensor for adenosine based on the quenching of Ru(bpy)(3)(2+)-doped silica nanoparticle ECL by ferrocene, Chem. Commun. 46 (2010) 7751–7753.
[33] Z. Wang, C. Lu, J. Liu, J.J. Xu, H.Y. Chen, An improved G-quadruplex DNAzyme for dual-functional electrochemical biosensing of adenosines and hydrogen peroxide from cancer cells, Chem. Commun. 50 (2014) 1178–1180.
[34] D. Wu, X. Ren, L. Hu, D. Fan, Y. Zheng, Q. Wei, Electrochemical aptasensor for the detection of adenosine by using PdCu@MWCNTs-supported bienzymes as labels, Biosens. Bioelectron. 74 (2015) 391–397.
[35] H.H. Huang, X.H. Yang, K.M. Wang, Q. Wang, Q.P. Guo, J. Huang, J.B. Liu, C.X. Song, Amplified fluorescence detection of adenosine via catalyzed hairpin assembly and host-guest interactions between β-cyclodextrin polymer and pyrene, Analyst 141 (2016) 2502–2507.
[36] J.K. Ahn, H.Y. Kim, S. Baek, H.G. Park, A new s-adenosylhomocysteine hydrolase-linked method for adenosine detection based on DNA-templated fluorescent Cu/Ag nanoclusters, Biosens. Bioelectron. 93 (2017) 330–334.
[37] R. Hu, X. Zhang, Q. Xu, D.Q. Lu, Y.H. Yang, Q.Q. Xu, Q. Ruan, L.T. Mo, X.B. Zhang, A universal aptameric biosensor: Multiplexed detection of small analytes via aggregated perylene-based broad-spectrum quencher, Biosens. Bioelectron. 92 (2017) 40–46.
[38] J. Shen, H. Wang, C. Li, Y. Zhao, X. Yu, X. Luo, Label-free electrochemical aptasensor for adenosine detection based on cascade signal amplification strategy, Biosens. Bioelectron. 90 (2017) 356–362.
[39] Z. Csoma, E. Huszar, E. Vizi, G. Vass, Z. Szabo, I. Herjavecz, M. Kollai, I. Horvath, Adenosine level in exhaled breath increases during exercise-induced bronchoconstriction, Eur. Respir. J. 25 (2005) 873–878.